J Appl Electrochem (2011) 41:1397–1406
DOI 10.1007/s10800-011-0361-5

ORIGINAL PAPER

Properties of electrodeposited silver–cobalt coatings

S. Nineva · Ts. Dobrovolska · I. Krastev

Received: 20 July 2011 / Accepted: 12 October 2011 / Published online: 27 October 2011

Abstract Silver–cobalt coatings were elecrodeposited from cyanide–pyrophosphate electrolytes with and without additives (diammonium oxalate monohydrate and 2-Butyne-1,4-diol). The deposition rate, the alloy composition, as well as some physicomechanical (internal stress, microhardness, plug-in forces, abrasion resistance) and electrical properties (contact resistance, magnetoresistance) of the obtained coatings, depending upon the applied current density or the cobalt content, respectively, were investigated. The increase in current density led to the increase in the Co content of the coatings and to a decrease in the grain size of both silver and cobalt phases. Granular structural type of deposits with a magnetoresistance of about 4% ratio was shown. The tensile stress observed in pure Ag deposits increased in the presence of Co and with an increase in its content in the alloy. The increase in the microhardness, abrasion resistance and electrical resistance of the Ag–Co coatings depended almost linearly on the Co content. The performed high speed electroplating showed significant increase in the deposition rate and smoothness of the coatings.

Keywords Electrodeposition · Electrolytes · Magnetoresistance · Properties · Silver–cobalt coatings

1 Introduction

In the last 20 years, the research interest in the electrodeposition of silver alloys with cobalt has been based on the expected magnetoresistive properties of the obtained material [1–5]. The investigations into the physicomechanical (it is well known that even traces of Co in the alloy increase significantly its microhardness and abrasion resistance), electrical (at higher content of Ag) and magnetic (at higher content of Co) properties of the alloy are not so numerous most probably because of the complicated processes of electrolysis and low stability of the electrolytes used [6, 7]. More than 40 years ago, a Russian group of researchers carried out investigations on the deposition of the silver–cobalt coatings and their properties depending on the electrolysis conditions [8]. There are no details about the quality of the coatings and the challenge of producing silver–cobalt coatings good enough for further investigation into their properties still exists.

Some investigations on the electrodeposition of silver–cobalt coatings have been reported in the last few years [6, 7, 9]. The literature survey has shown a limited number of appropriate electrolytes and lack of data about the coatings' parameters [6, 7]. The electrode processes and electrolysis conditions in cyanide–pyrophosphate electrolyte as well as the content and morphology of the produced silver–cobalt coatings have been presented earlier [6, 7, 9]. The analysis of the results showed the needs of additional investigations in order to produce coatings of good quality. The obtained coatings were compact but not homogeneous enough for reliable investigations into their properties (contact and abrasion resistance, etc.). For that reason, some additives were suggested and applied.

This paper represents a further study on the properties of different silver alloy systems previously investigated [10–13].

The aim of this paper is to study the properties of silver–cobalt coatings obtained from cyanide–pyrophosphate electrolytes with or without additives (diammonium oxalate monohydrate and 2-Butyne-1,4-diol).

S. Nineva (✉) · Ts. Dobrovolska · I. Krastev
Institute of Physical Chemistry, Bulgarian Academy of Sciences, 1113 Sofia, Bulgaria
e-mail: snineva@ipc.bas.bg

2 Experimental details

The composition of the electrolyte for the deposition of the alloy coatings is presented in Table 1. Distilled water and *pro analysis* grade reagents were used. The preparation procedure of the electrolyte is given elsewhere [6], and some of its electrochemical characteristics were discussed recently [9]. The electrolyte was not stirred.

The electrode processes of deposition and dissolution of the coatings were investigated by means of cyclic voltammetry. The experiments were performed in a 100 cm^3 glass cell at 50 °C without stirring of the electrolyte. The working electrode with an area of 1 cm^2 and two counter electrodes were made by platinum. Prior to each experiment, the platinum working electrode was etched in 50% HNO_3. A reference electrode Ag|AgCl (EAg|AgCl = 0.197 V vs. SHE) was used. At the time of the experiments, the reference electrode was placed in a separate cell filled with 3 M KCl solution (Merck), connected to the electrolyte cell by a Haber–Luggin capillary through an electrolyte bridge containing also 3 M KCl solution. The experiments were carried out by means of a computerized potentiostat/galvanostat (GAMRY Reference 600) using PHE 200, version 5.5 software (Gamry Instruments) with a sweep rate of 25 mV s^{-1}.

The coatings were deposited in a glass cell of 100 or 400 cm^3 at 50 °C, under both galvanostatic and potentiostatic conditions. The thickness of the deposited coatings was between 1 and 10 μm. Copper cathodes (2 × 1 × 0.03 cm or 7 × 1 × 0.03 cm) and platinum anodes were used. The preliminary preparation of the copper cathodes includes a standard procedure of electrochemical degreasing followed by pickling in a 20% solution of sulfuric acid. In order to avoid the contact deposition of silver, the cathode was immersed into the electrolyte under current.

Depending on the electrolysis conditions, the elemental composition of the coatings was determined by means of X-ray fluorescence analysis and by EDX.

The surface morphology was studied by means of scanning electron microscopy (SEM).

The jet-plating process was realized in a special experimental device (Jet–lab). The construction of the cell is described elsewhere [14]. The cathodes were brass sheets with a surface of 2.2 × 3.3 cm^{-2}, and the localized area for the deposition was 1.77 cm^{-2}. The coatings with a thickness of about 1–3 μm were deposited at room temperature at the flow speed of 200 and 600 L h^{-1}. The electrolyte was injected into the electrolyte cell through a titanium nozzle, connected as an anode.

The internal stress, IS, was monitored with the apparatus constructed by Stalzer [15] operating on the principle of the one-sided galvanized bendable cathode. The cathodes backsides were lacquer-insulated. Silver was deposited along 7 cm of the plate, dipped in the electrolyte (400 cm^3). During electrodeposition, the cathode is bending in a specific direction depending on the sign whether the induced internal stress is compressive or tensile. A sensor detects the deviation and compensates it through an electric feedback system. The force needed for compensation and hence the value of the internal stress is deduced from the electrical signal. The latter is transferred through a suitable interface to a computer for monitoring and processing. The method permits in situ monitoring of the internal stress during electrodeposition.

The signal is plotted as voltage versus time, and the stress is calculated according to the formula

$$S = K\frac{4\Delta UL}{3btd},$$

where S is the stress in the coating (N mm^{-2}); $K = 161$ mN V^{-1} is the apparatus constant; $L = 90$ mm is the distance between the contact point of the sensor on the sample and the level of the sample holder; $b = 10$ mm is the sample width; $t = 0.3$ mm is the thickness of the substrate; d is the thickness of the coating (μm).

The microhardness, H_v, of the deposited coatings was measured with the Polyvar apparatus using a load of 0.005 kp at different positions in the cross-sections of the deposits, and the average arithmetical value of these measurements was calculated.

The electrical contact resistance, R_Ω, of 6 μm thick layers was measured by the Burster Resistomat 2323

Table 1 Electrolyte composition

Components	Composition (g dm^{-3})					
	Electrolyte 1	Electrolyte 2	Electrolyte 3	Electrolyte 4	Electrolyte 5	Electrolyte 6
Ag as $KAg(CN)_2$	1	2	1	1	1	1
Co as $CoSO_4{\cdot}7H_2O$	5	15	5	5	5	5
$K_4P_2O_7$	100	300	100	100	100	100
$(NH_4)_2C_2O_4{\cdot}H_2O$	–	–	2	4	6	2
2-Butyne-1,4-diol	–	–	–	–	–	0.3
pH	9.2	9.2	8.9	8.8	8.7	8.9

microohmmeter on brass contact pins of diameter 4 mm and length 14 mm at a pressure force of 2 N. After the standard pretreatment (electrochemical degreasing, rinsing and neutralization), the pins were coated with the Ag–Co alloy. As reference samples, other gold-coated pins were used.

The plug-in forces, F, were measured during the introduction of contact pins coated with a 6-mm-thick deposit of Ag–Co alloy into pure silver coated jacks. For this purpose, the Zwick/Roell Z 2.5 apparatus was used.

The abrasion resistance, A, of the same layers was determined by the Bosch–Weinmann method using the samples from the measurements of the internal stress. In this method, an abrasive disk (diameter 47 mm, width 10 mm) moves under constant load (3.92 N) back and forth on the tested surface. After each cycle, the disk rotates in a small step, so as to provide fresh abrasive surface. By appropriate choice of the grain size of the abrasive band, it is possible to control the intensity of abrasion. In the present study, the latter was determined after 200 cycles using an abrasive band of grade 1,000. The abrasion resistance was determined by the weight loss. It is defined as the number of cycles required for the removal of 1 mm^3 of the tested material and is given by

$$A = z\left(\frac{D}{G}\right)$$

where A is the abrasion resistance (number of cycles for the removal of 1 mm^3 of the coating); D is the density of the material (mg mm^{-3}); z is the number of cycles; G is the weight loss (mg).

The magnetoresistance of the silver–cobalt coatings was measured by four-point method using "Lock-in" Amplifier SR510 of Stanford Research Systems (49 kHz, 1 μA). Magnetic field of 0.44 T (NdFeB) was applied on the sample perpendicular to the current. Copper foil of 40 μm thickness (PCB) was used as substrate and covered by 1 μm silver–cobalt coating (electrolyte 3, 0.4 A dm^{-2}, 2 C cm^{-2}) with composition of 20 wt% of cobalt. The free surface of the coating was attached to polypropylene foil and after that the copper foil was etched in $FeCl_3$. The calculations of magnetoresistance were made according to the formulae given in the paper of Hickley et al. [16]:

$$\mathrm{MR} = \frac{\Delta R}{R} = \frac{R(B) - R(0)}{R(0)},$$

or

$$\mathrm{MR}(\%) = \frac{\Delta R}{R} = \left[\frac{R(B) - R(0)}{R(0)}\right] \times 100,$$

where $R(B)$ is the resistance of the sample in magnetic field B.

3 Results and discussion

3.1 Deposition rate

The deposition rate dependence of the silver–cobalt coatings on the current density is nearly linear with one exception of the electrolyte 2 (Fig. 1) and varies from 0.01 to 0.30 μm min^{-1}. The deposition rate from electrolyte 2 is higher at the lower current densities (up to 1 A dm^{-2}), and then it shows almost stationary behavior with a decrease after 1.5 A dm^{-2}. The increase in the rate at the beginning is connected with the higher silver concentration in electrolyte 2. The deposition at higher current densities (1.5–2 A dm^{-2}) was connected with the destruction (black–brown precipitation) of the electrolyte, due to oxidation of pyrophosphate ions onto the anode as well due to the formation of non-soluble compounds during electrolysis. The quantity of 2 g dm^{-3} of the oxalate salt (electrolyte 3) results in significant increase in the range of working current densities as well as in a better homogeneity of the coating, but the deposition rate is close to the one showed and predicted from the behavior of the electrolyte 1. The further increase in the quantity of the oxalate salt (electrolytes 4 and 5) leads to some inhibition of the electrodeposition process and to lower deposition rate in comparison with electrolyte 3. The coatings from electrolyte 6 are deposited with the same speed as those from electrolyte 3.

3.2 Coating composition

The influence of the current density on the cobalt percentage in the coatings is shown on Fig. 2. The highest reached content of cobalt in the coatings is around 70 wt%. The cobalt content of the coatings obtained from electrolyte 1

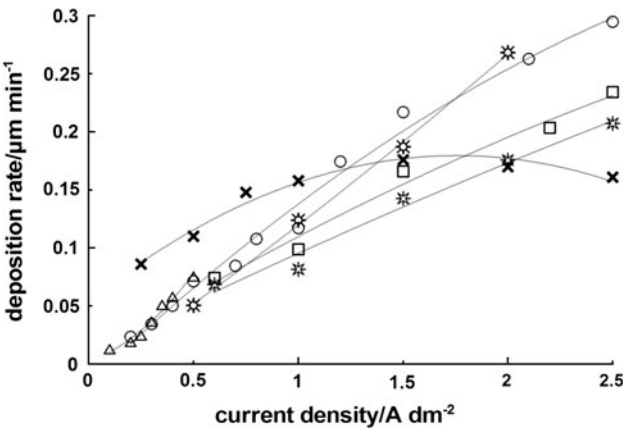

Fig. 1 Effect of the current density on the deposition rate of the Ag–Co coatings: electrolyte 1 (*triangle*), electrolyte 2 (*crossed*), electrolyte 3 (*circle*), electrolyte 4 (*square*), electrolyte 5 (*star*), electrolyte 6 (*sun*)

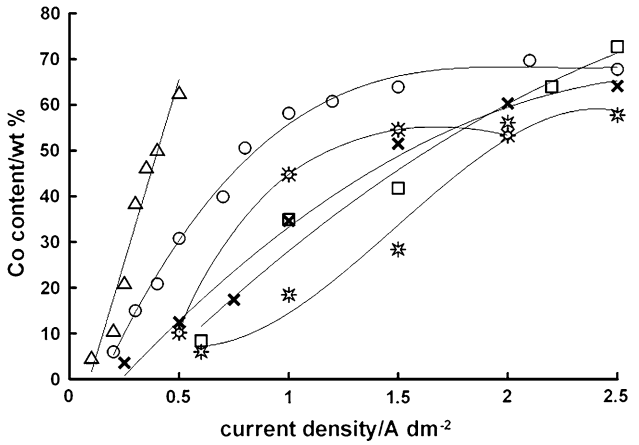

Fig. 2 Effect of the current density on the cobalt percentage in the coatings: electrolyte 1 (*triangle*), electrolyte 2 (*crossed*), electrolyte 3 (*circle*), electrolyte 4 (*square*), electrolyte 5 (*star*), electrolyte 6 (*sun*)

sharply increases to almost 65 wt% between 0.1 and 0.5 A dm^{-2}, and after 0.25 A dm^{-2}, the coatings are very heterogeneous. At current densities, higher than 0.5 A dm^{-2}, thin dark blue-to-green film of cobalt hydroxide covers the coating.

The increase in the silver concentration in the electrolyte 2 as well as the increase in the range of applied current densities results in the deposition of coatings with the same cobalt content at higher current densities.

The addition of the proposed organic substances to electrolyte 1 (electrolytes 3, 4, 5, 6) leads to a better appearance of the coatings, possibly due to the suppressing of the alkalization and by this way preventing the formation of passive films of cobalt hydroxide onto the cathode during electrolysis.

Based on the electrodeposition results (Figs. 1, 2), the coatings' properties were mostly investigated on coatings obtained from electrolyte 3. Sometimes, they were compared with those of coatings obtained from electrolyte 1. Electrolyte 3 assures a broad range of working current densities and allows the deposition of smoother and homogeneous coatings.

Figure 3 shows the cyclic voltammetry curves, obtained in electrolytes 1 and 3. The deposition process in both electrolytes starts with the deposition of silver with a maximum at the potential of −350 mV (Fig. 3, Inset a). The co-deposition of cobalt starts after −950 mV and at the potential of −1,025 mV reaches the maximum of the reaction rate of alloy formation (Fig. 3, Inset b).

The influence of the oxalate ions could be related to two different effects. The first one is connected with the specific adsorption typical for organic compounds as the oxalate [17] that leads to refined grain sizes of the crystals. Silver and cobalt are almost immiscible [18], and oxalate reduces the size of the crystals of the separate metals due to their suppressed growth and the increase in the nucleation rates. The second effect is due to the buffer agent characteristic of the ammonium ions from the oxalate salt, which leads to the prevention of alkalization of the solution near the electrode-solution interface, which was confirmed by EDX-analysis (Oxygen was not detected in the coatings deposited in the presence of diammonium oxalate in the electrolyte, respectively, in the absence of this additive several atomic percents of oxygen were registered). As a result, the earlier start of the hydrogen evolution reaction in the case of the electrolyte containing oxalate (Fig. 3, dashed line) is well defined. This second effect is directly

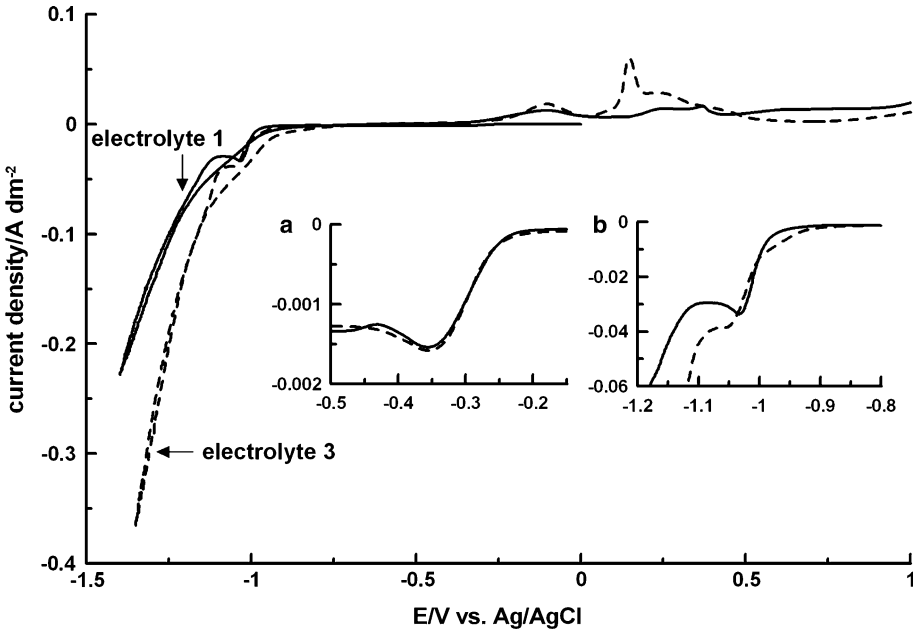

Fig. 3 Cyclic voltametric curves in different electrolytes: electrolyte 1 (*solid line*) and electrolyte 3 (*dashed line*); *Insets a* silver deposition peak; *b* cobalt deposition peak

connected with the cobalt deposition process from pyrophosphate complexes. In another paper [9], the effect of alkalization in the vicinity of the cathode, during the simultaneous cobalt deposition and hydrogen evolution, was explained as a reason of the well-defined peak in the CV curve of the electrolyte 1 (Fig. 3b). The local alkalization affects strongly the stability of the pyrophosphate complexes of the cobalt ions near to the cathodic surface (they are not stable at higher pH values).

In the anodic part, a hump between potentials –0.25 to 0 V, which belongs to the dissolution of the cobalt and a second, split peak that represents the dissolution of the silver is observed [9]. There are some differences in the shapes of the second peak (in the range of 0 to +0.25 V) in electrolytes 1 and 3, most probably due to the presence of free ammonium ions originated from the oxalate salt, which act here as additional ligands to the cyanide ones in the formation of complexes during the silver dissolution.

The alloy composition dependence on the potential is presented on Fig. 4. There is no significant difference in the composition of the coatings obtained from electrolyte 1 and electrolyte 3 under potentiostatic conditions. In the potential interval between −0.98 and −1.08 V (100 mV), there is an increase in the cobalt content from 2 up to 60 wt%. This behavior is in good agreement with the cyclic voltammetry curves presented earlier. The highest Co content of the coatings from both electrolytes has been reached at the potentials of −1.08 V.

3.3 Phase composition of the coatings

X-ray diffractograms of the pure metal coatings, obtained in electrolyte 1 in the absence of cobalt or silver, are shown on Fig. 5a and b, respectively. In comparison with the silver, the cobalt coating has a poorer crystal structure with small intensity and broad peaks of the presented phases. The cobalt coatings consist of two phases (α and β-cobalt).

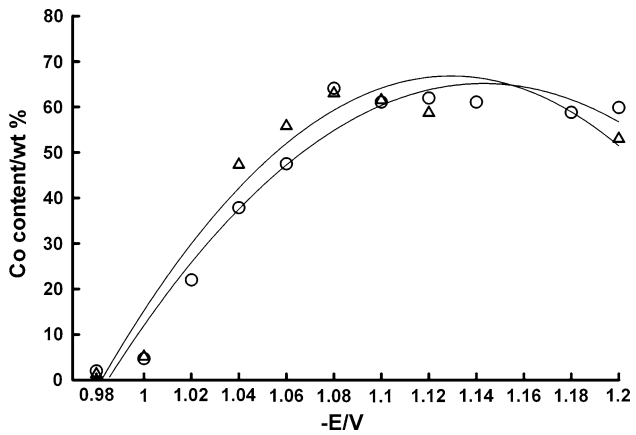

Fig. 4 Effect of the potential on the cobalt percentage in the coatings: electrolyte 1 (*triangle*), electrolyte 3 (*circle*)

The equilibrium phase diagram of Ag–Co shows that this system is of a mutually insoluble type at ambient temperature [19] and is separated into pure Ag and Co phases. The X-ray diffractograms in Fig. 5c and d present the data for the electrodeposited Ag–Co coatings from electrolytes 1 and 3, and they are in good agreement with those for Ag–Co coatings obtained from other electrolytes [2, 20]. Peaks of the copper substrate appear in some diffractograms. The diffraction peaks of the pure silver are broadened with increasing Co content at corresponding increase in the current density. This indicates that the grain size becomes smaller with alloying. In the investigated composition range, up to 68 wt% cobalt, no diffraction peaks of Co metals appeared. It could be assumed that the increase in the current density, i.e., the increase in the cobalt content in the coating, results in smaller grains of the Ag-phase (matrix) and in precipitation of smaller Co grains or particles in the coating (at higher current densities) [2]. The size of the Co grains in the Ag matrix in the coatings with no more than 30 at.% Co is of a big importance for the magnetoresistive (MR) properties of this system. There is an optimal particle size required for the highest MR ratio [16].

3.4 Internal stress

In silver coatings, electrodeposited from cyanide electrolytes, low positive (tensile) internal stress, IS, is observed [12]. The tendency of changes in the IS during the electrodeposition of silver from cyanide–pyrophosphate electrolyte illustrated in Fig. 6a is similar. The increase in the current density causes rise in the IS of the silver coatings. The pure cobalt coatings from the pyrophosphate ions containing electrolytes show higher IS than these of pure silver (Fig. 6a). During the Ag–Co co-deposition (Fig. 6b), from almost stress-free (low compressive stress) coatings (1 wt% Co; -1.2 N mm^{-2}) to stressed (high tensile stress) coatings (60 wt% Co; 13.6 N mm^{-2}) are observed. The increase in the current density leads to an increase in the Co content and to a decrease in the grain size of the crystalites (part 3.3). The coatings with more than 10% Co have significant tensile stress which is also typical for pure Co coatings deposited at higher current densities. The electrodeposited coatings from electrolyte 3 show the expected behavior due to the increase in the current density and, respectively, the increase in the Co content in deposits.

3.5 Contact resistance

The contact resistance, R_Ω, was measured against a gold-plated substrate or samples of the same composition. It increases at higher current densities, i.e., at a higher Co

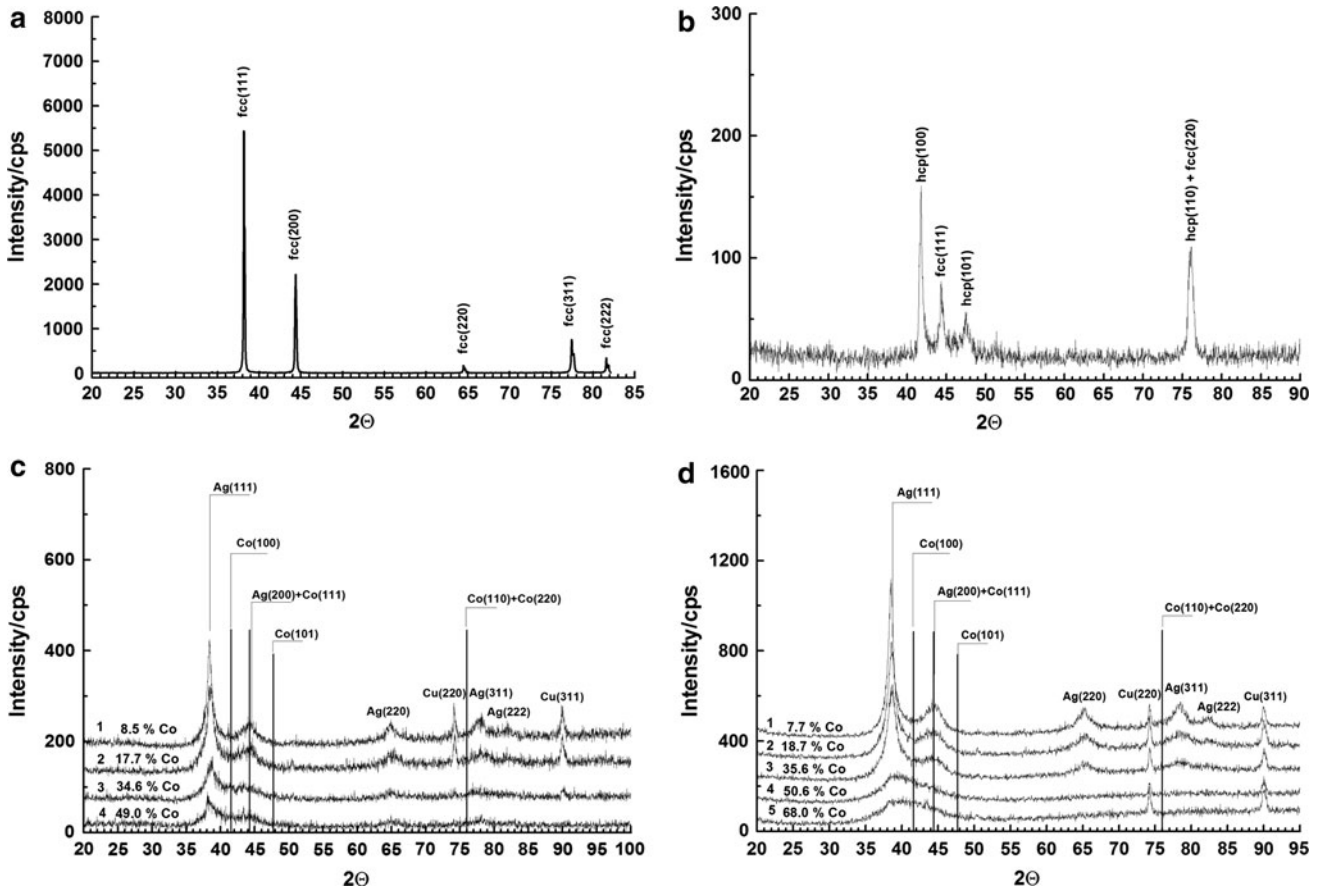

Fig. 5 **a** X-Ray diffractogram of pure Ag coating obtained in electrolyte 1. **b** X-ray diffractogram of pure Co coating obtained in electrolyte 1. **c** X-ray diffractograms of Ag–Co coatings with different cobalt content, obtained in electrolyte 1. **d** X-ray diffractograms of Ag–Co coatings with different cobalt content, obtained in electrolyte 3

content in the deposit. The contact resistance of the coatings with Co content up to 20 wt% from electrolyte 1 is about 1 mΩ and reaches 9.5 mΩ at 50 wt% Co. In the case of coatings obtained from electrolyte 3, the contact resistance of deposits with up to 20 wt% Co has the same values as those in the coatings from electrolyte 1. With the increase in the cobalt content up to 65 wt% in the coatings from electrolyte 3, the contact resistance increases up to 3.7 mΩ, which is much less than the resistance measured in the coatings from electrolyte 1. This effect could be related to the achieved homogeneity of the coatings obtained in electrolyte 3. The values of the contact resistance measured against gold are lower, as expected.

3.6 Plug-in forces

The effect of the Co content on the plug-in forces of the Ag–Co coatings from electrolyte 3 is shown on Fig. 7. The plug-in forces increase with the increase in the Co content of the coatings. In comparison with the investigated other alloys of silver (Ag–Sb, Ag–Bi, Ag–In, Ag–Sn), the Ag–Co alloy does not show lubricating properties.

3.7 Microhardness

In comparison with the microhardness, H_v, of the pure silver coating deposited in the absence of cobalt from electrolyte 3, which is around 600 N mm^{-2}, the coatings with 7 wt% of Co are three times harder. There is almost linear dependence between Co content and the microhardness of the coatings. Coatings with 56 wt% Co show microhardness of 3,108 N mm^{-2} (Fig. 8). The cobalt deposition as alloying element in the production of hard coatings and alloys is widely applied in practice. The highest microhardness observed in this system at 56 wt% corresponds to the microhardness of electrodeposited pure cobalt coatings [21].

3.8 Abrasion resistance

The electrodeposited Ag–Co coatings have a predictable, due to the cobalt co-deposition, increase in the abrasion resistance with the increase in the current density, i.e., in the Co content of the coating. The dependency is almost

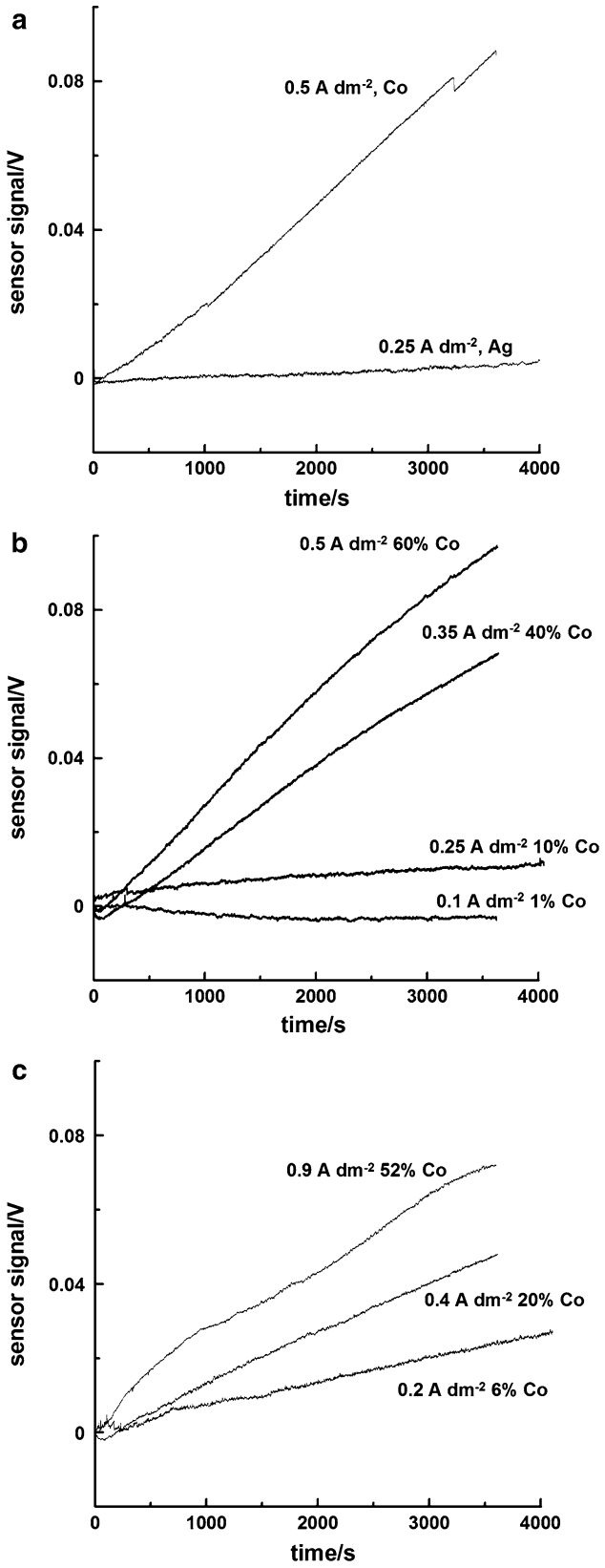

Fig. 6 Sensor signal during *IS* measurements in: **a** Ag and Co electrolytes (one metal only) at different current densities. **b** Ag–Co co-deposition from electrolyte 1. **c** Ag–Co co-deposition from electrolyte 3

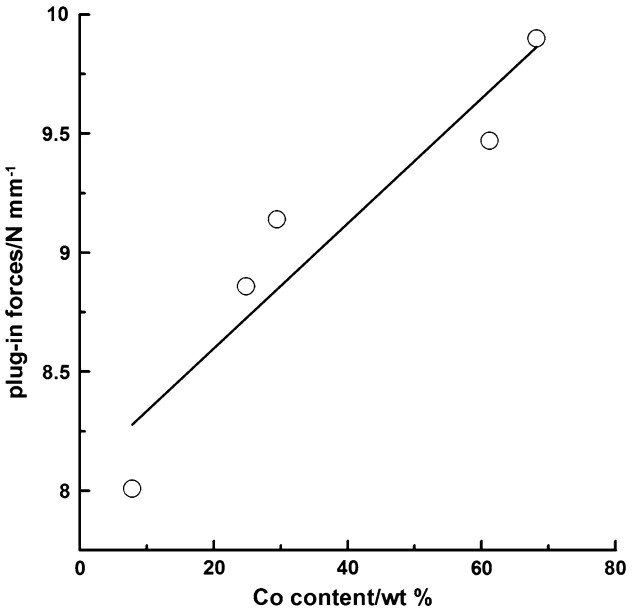

Fig. 7 Effect of the Co content on the plug-in forces of Ag–Co coatings from electrolyte 3

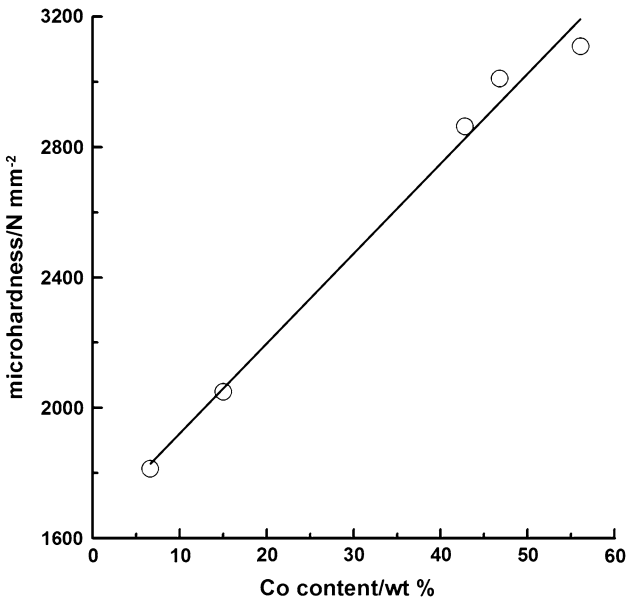

Fig. 8 Effect of the cobalt content on the microhardness (H_v) of the Ag–Co coatings from electrolyte 3

linear (Fig. 9) and the abrasion resistance increases in the investigated range of the current density or cobalt content, in contradiction to the cases of alloy coatings of silver with other "softer" metals, like Bi, In, Sb, etc. [13].

3.9 Magnetoresistance

The preparation of the sample and the graph of the magnetoresistance, MR, measurement are illustrated in Fig. 10.

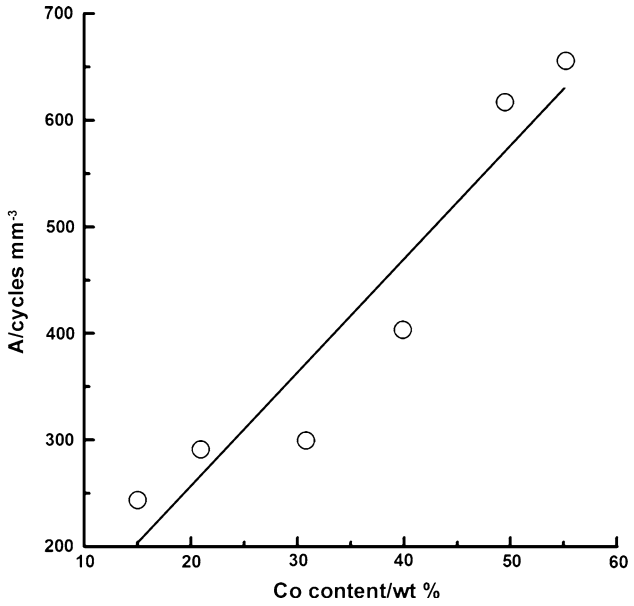

Fig. 9 Effect of the cobalt content on the abrasion resistance of Ag–Co coatings from electrolyte 3

The procedure is described in the experimental part of this study. The measurement of the electrical resistance is performed before and after applying the magnetic field. The observed effect of the change in the MR of the sample is 4%. This ratio is higher than expected for a galvanostatic co-deposited. In case of the magnetic field applied parallel to the direction of the current, no difference in the MR ratio has been observed. This is a typical MR characteristic of samples of granular (isotropic) materials [1]. The results show the promising magnetoresistive properties of the electrochemically obtained Ag–Co coatings.

3.10 High speed electrodeposition process

High speed electroplating has a lot of beneficial characteristics. This process allows the use of low metal concentration electrolytes and a big increase in the deposition rate. In the case of Ag–Co coatings of about 1 μm thickness and further investigations on some interesting for the electronics properties, such as MR, the high speed electroplating is an important technique. By using the high speed process, the deposition rate has been increased up to ten times (at the same Co content of the coating)—from 1 to 3 μm min^{-1}, during deposition from the two investigated electrolytes 1 and 3. The changes in the Co content, during the deposition from electrolyte 1 and 3, for different current densities, at two different flow rates (200 and 600 dm^3 h^{-1}) are illustrated in Fig. 11a and b.

The increase in the flow rate favors the Ag deposition as could be expected due to its more positive deposition potential. The Co content in coatings obtained at the same current densities decreases with the increase in the flow rate. The optical appearance of the coatings from electrolyte 3 is characterized with better homogeneity and brightness in the whole range of current densities, both during deposition in the high speed and normal plating processes.

Figure 12 shows images of Ag–Co coating surfaces. They illustrate the difference between the surface of the

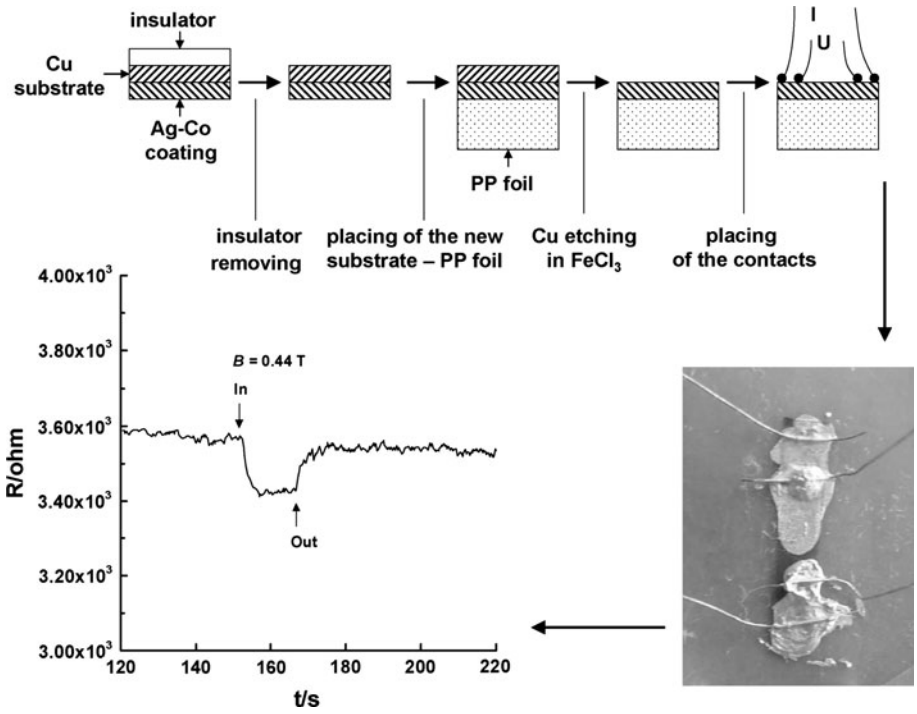

Fig. 10 Schematic illustration of the sample preparation for *MR* investigations and the graph of the electrical resistance measurement

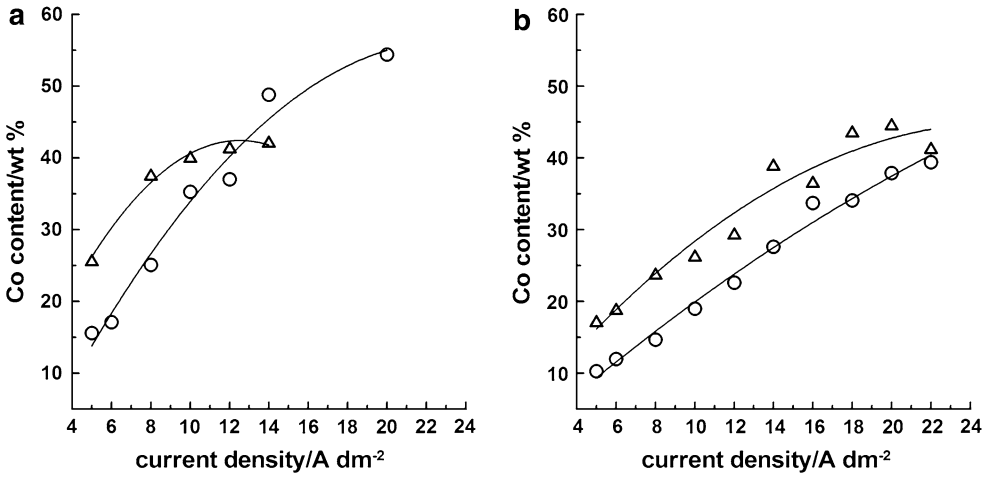

Fig. 11 Effect of current density on the cobalt percentage in the coatings: electrolyte 1 (*triangle*) and electrolyte 3 (*circle*) during high speed electroplating: **a** 200 $dm^3\ h^{-1}$, **b** 600 $dm^3\ h^{-1}$

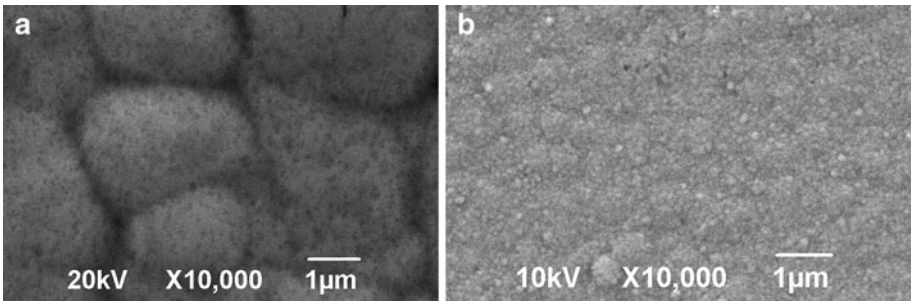

Fig. 12 SEM images of Ag–Co coatings with 20 wt% of Co from electrolyte 3 obtained in: **a** normal plating process, **b** high speed plating process

coatings from one electrolyte (3) obtained under different conditions: normal (a) and high speed plating (b). The size of the crystallites visible decreases in the high speed plating process, because of the higher current densities used, far from equilibrium, which results in a higher nucleation rate.

4 Conclusions

The investigations on the Ag–Co co-deposition show the possibility to obtain coatings with the desired composition depending on the electrolysis condition and on small changes in electrolyte composition. The small amount of oxalate ions improves significantly the homogeneity of the deposits and expands the range of working current densities. The increase in current density leads to the increase in the Co content of the coatings and to a decrease in the grain size of both silver and cobalt phases. Coatings with granular structure with a magnetoresistance of about 4% can be deposited from the investigated electrolyte.

The tensile stress observed in pure Ag deposits increases with the increase in Co content as well as with the increase in the current density due to the alloy formation and the refined size of the grains of the deposits. The increase in the microhardness, abrasion resistance and electrical resistance of the Ag–Co coatings depends almost linearly on Co content in the coatings.

The results of the high speed electroplating show a significant increase in the deposition rate and smoothness of the coatings, and a possibility for application of the suggested electrolyte 3 in high speed deposition plants.

Acknowledgments The authors are thankful to Prof. S. Tinchev (Institute of Electronics, Bulgarian Academy of Sciences) for the measurements of the MR properties of the Ag–Co coatings, to Deutsche Forschungsgemeinschaft (DFG) (Project 436 BUL 113/97/0-4) and to Umicore Galvanotechnik GmbH for the given possibility to perform experiments using the Jet-Lab equipment.

References

1. Xiao JQ, Jiang JS, Chien CL (1992) Phys Rev B 46:9266
2. Zaman H, Ikeda S, Ueda Y (1997) IEEE Trans Magn 33:3517
3. Fedosyuk VM, Kasyutich OI, Schwarzacher W (1999) J Magn Magn Mater 198:246
4. Kenane S, Chainet E, Nguyen B, Kadri A, Benbrahim N, Voiron J (2002) Electrochem Commun 4:167
5. Garcia-Torres J, Valles E, Gomez E (2011) Mater Lett 65:1865
6. Nineva S, Dobrovolska T, Krastev I (2008) Bulg Chem Com 40:248
7. Nineva SL, Dobrovolska TV, Krastev IN (2011) Bulg Chem Com 43:88

8. Vjacheslavov PM, Grilihes SJ, Burkat GK, Kruglova EG (1970) Galvanotechnika Blagorodnih i Redkih Metallov. Mashinostroenie, Leningrad, pp 5–52
9. Nineva SL, Dobrovolska TV, Krastev IN (2011) Bulg Chem Com 43:96
10. Krastev I, Petkova N, Zielonka A (2002) J Appl Electrochem 32:811
11. Krastev I, Valkova T, Zielonka A (2004) J Appl Electrochem 34:79
12. Krastev I, Dobrovolska T, Kowalik R, Zabinski P, Zielonka A (2009) Electrochim Acta 54:2515
13. Hrussanova A, Krastev I, Beck G, Zielonka A (2010) J Appl Electrochem 40:2145
14. Wingenfeld P (2004) Galvanotechnik 95:879
15. Stalzer M (1964) Metalloberflache 18:263
16. Hickey BJ, Howson MA, Musa SO, Wiser N (1995) Phys Rev B 51:667
17. Purin BA (1975) Elektroosujdenie metalov iz pirofosfatnih elektrolitov. Zinatne, Riga, pp 87–96
18. Hansen M, Anderko K (1958) Constitution of binary alloys. McGraw-Hill Book Company, New York, pp 16–17
19. Predel B. In: Madelung O (ed) Springer materials—the Landolt-Börnstein Database. (http://www.springermaterials.com). doi: 10.1007/10000866_20
20. Watanabe T (2004) Nano-plating. Elsevier, Amsterdam, pp 387–397
21. Bubialis Yu (1969) In: Matulis Yu (ed) Blestiaschie elektrolitiecheskie pokritija. Mintis, Vilnus, pp 250–255